Applied Energy 334 (2023) 120621

Contents lists available at ScienceDirect

Applied Energy

journal homepage: www.elsevier.com/locate/apenergy

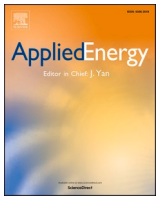

Quantum computing for future real-time building HVAC controls

Zhipeng Deng, Xuezheng Wang, Bing Dong *

Department of Mechanical & Aerospace Engineering, Syracuse University, Syracuse NY13244, United States

HIGHLIGHTS

- We used quantum computing to optimize model predictive control of building HVAC systems.
- We formulated mixed-integer non-linear programming as quadratic unconstrained binary optimization for quantum computer.
- Solution of quantum computing was almost the same as traditional optimization method, but computing time was greatly reduced.
- Quantum computing had the potential to solve large-scale non-linear optimization problems for building energy systems.

ARTICLE INFO

Keywords:
Discrete optimization
Mixed-integer programming
Quadratic unconstrained binary optimization
Quantum annealing
Energy-efficient building

ABSTRACT

Buildings contribute to more than 70% of overall U.S. electricity usage and greenhouse gas (GHG) emissions. HVAC systems in buildings often consume more than 40% of the total building energy usage. To reduce such high energy use, numerous control strategies including optimal and predictive controls have been developed and demonstrated. To achieve a near real-time solution, most previous research has simplified the non-linearity of building thermodynamics and provided an approximate optimal solution. The future HVAC control optimizes more connected devices in buildings, which requires a rapid and accurate response, not only to the building itself but also to the grid signals. It also poses the challenge of solving non-linear problems with discrete variables. With the recent development of quantum computers, this has become feasible. In this paper, we developed a new optimization solution based on quantum annealing for model predictive control (MPC) of a rooftop unit (RTU). Compared to traditional optimization methods, we obtained similar solutions with less than 2% differences and improved computational speed from hours to seconds. We also demonstrated an 80% reduction in total electricity consumption and a 21% reduction in electricity bills by considering day-ahead price time-of-use demand response signals. Quantum computing has proven capable of solving large-scale non-linear discrete optimization problems for building energy systems.

1. Background

By 2050, a staggering 70 % of the world's population is projected to live and work in cities [1], while two-thirds of global primary energy consumption will be attributed to cities, leading to the production of 71 % of the global direct energy-related greenhouse gas (GHG) emissions [2]. People currently spend more than 90 % of their time in buildings, which contributes to more than 76 % of overall U.S. electricity usage [3]. Such GHG emissions contribute to climate change, which is one of the most dominant forces shaping the Earth system and the greatest challenges of our generation. Many globally recognized environmental and climate threats such as heat stress, abrupt cold snap, air pollution, water scarcity, and energy insecurity are either rooted in or exacerbated by the uniqueness of the urban environment. With the aging of the US building stock, grid, and urban infrastructure, climate threats are expected to further intensify due to the rapid urban development coupled with climate change.

In the US, space heating accounted for 38 % of the energy delivered in buildings, far more than any other end-use. Meanwhile, electricity used for space cooling by residential and commercial sectors accounted for 10 % of total US electricity consumption in 2020 [4]. Advanced building controls have demonstrated 20–80 % energy savings through literature [5,6]. It also offers a vast potential for sustainable buildings [7]. With energy-saving and sustainability requirements, we need optimal control for the building HVAC systems.

Currently, proportional-integral (PI) controllers are widely used in

* Corresponding author.
E-mail address: bidong@syr.edu (B. Dong).

https://doi.org/10.1016/j.apenergy.2022.120621
Received 22 June 2022; Received in revised form 23 December 2022; Accepted 28 December 2022
Available online 21 January 2023

building automation systems for their simplicity and robustness to achieve conditioned indoor environments [8]. However, it only responds to current sensor readings without consideration of any other effects as reactive control. In buildings, there are complex heat transfers and the lagging effects due to the thermal mass of envelopes and indoor sources. They will increase the demands of load on the HVAC system and lead to a waste of energy [9]. Therefore, a good control strategy is needed to take into account the thermal effects of the buildings and reduce the energy usage while maintaining indoor comfort. Originated from advanced process control, model predictive control (MPC) can capture the dynamics of the building systems [10]. Predictions are derived with the information from the physical devices, thus the optimal control can be applied to systems with well-defined constraints. The features of MPC make it more prevalent in power system control. With the development of computing tools, MPC is getting more and more attention in the field of building energy [11]. Modeling and optimization can play an important role in the sustainable energy systems of buildings [7]. However, most of the real-time MPC case studies for building HVAC system have the following characteristics that prevent large-scale and robust deployment: difficulty in achieving real-time MPC, inaccuracy due to simplified non-linear models, and inefficient solver for discrete variables.

1.1. Difficulty in achieving real-time MPC

First, with the uncertainties of the weather forecast [12–14], occupancy level [12,15,16], and real-time energy pricing [17–20], the MPC required real-time response to update the control operations. It was necessary to solve the optimization problem within the control time step, such as 15 min. But it is very difficult to achieve real-time MPC for building HVAC systems. Many researchers have attempted to develop real-time MPC to reduce the energy use by building HVAC systems, such as air handling units (AHU), heat pumps, and variable air volume (VAV) systems [21]. For example, Schirrer et al. [22] developed a real-time non-linear MPC for a low-energy office building consisting of the heat pump and solar collector. Even for a 30 % variation in weather prediction, it showed good control performance and robustness. Joe and Karava [23] proposed an MPC strategy to optimize the performance of radiant floor heating and cooling systems in office buildings. The electricity use of the chiller was three polynomials. They found that the controller could save 29–50 % of energy compared with a baseline air delivery system. Asad et al. [24] developed multiplexed real-time optimization for non-linear dynamics of AHU and achieved 10 % energy savings. Ganesh et al. [25] used a mass balance model and built a dynamic optimization strategy of AHU for the control of indoor air pollutants. The optimization reduced the pollutant concentration by 31 % and energy use by 17.7 %. For a building with many thermal zones, the optimal control design for HVAC system will have a large number of control variables, in particular, discrete variables (e.g. fan status). This causes the search space increasing exponentially, resulting in an NP-hard problem. Hilliard et al. [26] implemented MPC with zone-based thermal comfort adjustments for an academic building. The experiments showed a 29 % reduction in HVAC electricity. Brooks et al. [27] developed an occupancy-based energy-efficient MPC for multiple rooms and showed energy savings potential of 29–80 %. Li et al. [28] decomposed the multi-objective optimization of thermal comfort, air quality, and energy use for VAV systems. It effectively found the proper trade-off between maintaining thermal comfort and indoor air quality, and the energy use was only 2 % higher. Bengea et al. [29] presented field experiment results of MPC, which optimized the operation of VAV serving a commercial building. Their demonstration results showed energy savings of 20 % during the transition season and 70 % during the heating season. Based on the literature review, the main challenge to achieve real-time MPC is the computational algorithm to solve the optimization part of a MPC within one control step (e.g 15 min). In order to achieve real-time, prior research studies simplified nonlinear control models to be a continuous and linear, and solved within a short control step [30], or a discrete linear problem that can be solved by mix-integer programming quickly as well [31]. None of prior studies were a non-linear optimization problem with discrete variables and implemented in real-time.

1.2. Inaccuracy due to simplified non-linear models

Second, most energy systems in buildings were complex and non-linear systems. The non-linearity of the system made the optimal control difficult, and the optimization results could be inaccurate due to the simplified models. For optimizing the complex non-linear building HVAC systems, previous approaches included multi-stage and multi-level optimization [19,17,32], decomposed, distributed, and decentralized optimization [33,34,18], agent-based method [34,19,13], local approximation and linearization [20,35,36]. These methods could not only convert and solve non-linear problems, but also accelerate the computation. For example, Cigler et al. [37] outlined an approximation of non-linear optimal control for the predicted mean vote index and obtained an additional 10–15 % of energy-saving potential. Drgoňa et al. [38] developed MPC by decoupling of non-linearities for a ground-source heat pump in an office building and saved 53.5 % of energy. However, these existing approaches to speed up the computation may lack of accuracy due to simplified non-linear models. Recently, some studies have used machine learning models to solve optimal control for complex building HVAC systems [39,40,41,5]. Such models were easy to build, even for a very complicated system. So that machine learning models could achieve real-time control. But for the robustness of these models in varied environments, the verification from previous studies using the machine learning method was only implemented for one or a few days.

1.3. Inefficient solver for discrete variables

In addition, optimization of building HVAC systems usually involved many discrete variables, such as whether to use a system component, operating status as on or off, and hierarchical stage control. Current optimization solvers were inefficient for complex problems with many discrete variables. The traditional approach for the optimization of discrete variables was typically a search algorithm [41]. In recent years, mixed-integer linear programming (MILP) and mixed-integer non-linear programming (MINLP) have received increasing attention from both academia and industry [42]. Deterministic algorithms for solving large-scale problems were needed to deal with growing subproblem sizes and exponential growth of branch-and-bound trees. In this case, it led to the enumeration of solution alternatives in the feasible space. This method could not deal with the optimization of a complex system in real-time [43]. In addition, *meta*-heuristics techniques, such as simulated annealing [44], particle swarm optimization [45,46], and genetic algorithm (GA) [47–49] also became popular nowadays, due to their ease of implementation and low requirement for prior knowledge of the optimization problem. However, these techniques could only solve unconstrained optimization problems. They could not strictly find the global optimum, either [50]. For complex problems that were hard to converge, multiple runs were required to find a better solution. Previously, GA was used to optimize the building HVAC system [51]. People also formulated the optimization of building HVAC systems and net-zero energy building into MILP, and used Gurobi and CPLEX software to solve [52,53]. These traditional optimization methods for large-scale energy systems required a very high computational effort [54]. With the increasing complexity of the problem and more discrete variables to be optimized, it typically required exponential computing time [55]. Finally, the most common technique used to solve real-time building energy management problems was convex optimization. For linear optimization, MILP, and quadratic programming, due to the simplicity and convexity, a global solution was guaranteed [6]. Non-linearity of

complicated energy systems also made formulating the control strategy very hard [56]. In many engineering optimization problems, the non-convexity of the problem made it impossible to obtain a globally optimal solution [6].

Through the literature review, we found that developing real-time MPC of a non-linear system for mixed-integer discrete optimization was very challenging. The research gap and challenges are that few previous studies could find the optimal control for the complex non-linear systems with discrete variables within an acceptable computing time. In order to increase the efficiency and reliability of the energy system at a building or building clusters level, it is imperative to optimally manage and control a large number of smart devices for future smart buildings and communities. Hence, we needed a better computational tool to solve these optimization problems.

The purpose of this study was to apply quantum computing (QC) to optimize energy efficiency through developing a non-linear MPC with discrete variables for building HVAC system. Specifically, we formulated the MPC optimization of a rooftop unit (RTU) into a quadratic unconstrained binary optimization (QUBO) problem. To verify the feasibility, then we used a quantum computer to solve such an optimization problem and obtained the results successfully. At last, we also compared the results and computing time of quantum computing with traditional optimization methods.

2. Quantum computing

Quantum computing uses quantum mechanics to solve problems that are too complicated for conventional computers. For example, it uses qubits that can represent 0/1 at the same time to compute, so the computational speed can increase exponentially with the number of qubits. Quantum computing has recently attracted more attention due to its unique ability that was different from conventional computers in terms of computational principles and speeds. The circuits in a quantum computer obeyed quantum mechanics. The basic unit of a quantum computer was the qubit. A qubit could be in a quantum state of 1 or 0, or a superposition of the two states. However, when it was measured, it was either 0 or 1; the probability of either outcome depended on the quantum state of qubits immediately before the measurement [57]. Another property of qubits was the ability to form entangled states, allowing to form relationships between separated random behaviors. Quantum computers used these characteristics of the qubit to carry out computations.

Since the computational principle of the quantum computer was different from that of conventional computers, it provided a novel approach to solving some complex problems with significant speed advantages [58,59]. For example, Shor [60] proposed the quantum algorithm for factorization of large numbers, which was exponentially faster than any classical algorithm. Due to the potential applications of cryptography, it greatly motivated the development of quantum algorithms. Grover's search algorithm [61] was able to search large databases in the square root of complexity time. Harrow et al. [62] developed a quantum algorithm for solving linear systems of equations. Inspired by these algorithms, many researchers have developed numerous quantum algorithms for further applications, such as data fitting [63], clustering [64], and solving linear differential equations [65].

To solve optimization problems, quantum annealing and adiabatic quantum computation relied on the adiabatic theorem. People have built quantum annealers in recent years [66]. In the system, it was initialized in the lowest energy eigenstate of the Hamiltonian. Hamiltonian was a mathematical description of a physical system in terms of energy, corresponding to the objective function of an optimization problem [67]. The slow annealing process evolved the quantum state into a user-defined problem. By reducing the Hamiltonian of the system from a large value to zero, the system was driven to its optimum state as the eigenstate of the quantum Hamiltonian. It could be used for searching for optimal solution space effectively [68]. Quantum Hamiltonian in Ising formulation could be expressed as

$$H_{ising} = -\frac{A(s)}{2}\sum_i \widehat{\sigma}_x^{(i)} + \frac{B(s)}{2}\left(\sum_i h_i \widehat{\sigma}_z^{(i)} + \sum_{i>j} J_{ij}\widehat{\sigma}_z^{(i)}\widehat{\sigma}_z^{(j)}\right) \tag{1}$$

where $\widehat{\sigma}$ was Pauli matrices operating on a qubit q_i, $A(s)$ the tunneling energy at annealing fraction s, $B(s)$ the Problem Hamiltonian energy at annealing fraction s, h_i the self-interaction energy on a qubit. J_{ij} the coupling energies between spins.

Compared to the traditional optimization algorithm like ant colony optimization algorithm [69], GA [47], and simulated annealing [44] to find optimal values, quantum annealing was a more powerful method. It allowed quantum tunneling, which gave an increasing likelihood of reaching the ground state under the same conditions of annealing schedule and interaction. It assisted in escaping the local minimum and enabled the search for the global minimum [70]. The recent development of hardware and algorithms of quantum annealer has given people the opportunities to solve extremely complex optimization problems, even NP-hard problems [67]. To solve an optimization problem using quantum annealing, we first needed to formulate it as unconstrained optimization. With the properties of qubits, then we needed to formulate the continuous or discrete optimization variables into binary variables. When the objective function was a polynomial of variables, it was polynomial unconstrained binary optimization (PUBO), which was a subset of binary optimization as

$$H(\boldsymbol{x}) = \sum_S C_S \prod_{i\in S} x_i \tag{2}$$

where $x_i \in \{0,1\}$.

The quantum annealer could solve QUBO problem, where the order of the polynomial in Eq (2) was two that

$$H(\boldsymbol{x}) = \sum_i C_i x_i + \sum_{i,j} C_{ij} x_i x_j \tag{3}$$

where $x_i, x_j \in \{0,1\}$.

The first part was linear, and the second part was quadratic and non-linear. Its form was the same as the quantum Hamiltonian in Eq (1), thus we could map the QUBO problem into the quantum processing unit (QPU) and solve it by quantum annealing.

Recently, some researchers were trying to develop algorithms and utilize quantum annealers to resolve optimization problems, especially complex multivariable optimization [71]. For example, Ajagekar and You [72,73] developed novel quantum computing-based hybrid solution strategies for molecular design and facility location-allocation for energy systems infrastructure development, unit commitment of electricity power systems operations, and heat exchanger network synthesis. Ding et al. [74] applied quantum annealing for network design and analysis. Castillo et al. [75] optimized the refinery scheduling process with a quantum annealer. Quantum annealing could also optimize the power network [76,77] and water distribution network [78]. The optimization's outcomes were deemed to be quite positive. At last, the quantum annealer also had the potential to solve more problems, such as the optimization of machine learning models [79–81]. However, quantum computing method has never been used for optimizing the model predictive control of building HVAC systems. The possible reasons are as follows. At first, prior studies often relied on a continuous and linear MPC optimization problem [30], or a discrete linear problem that can be solved by mix-integer programming [31]. On the other hand, a practical quantum computer has not been available in the past years.

3. Methodology

3.1. General MPC problem for building HVAC systems

The general MPC formulation for the building HVAC systems can be

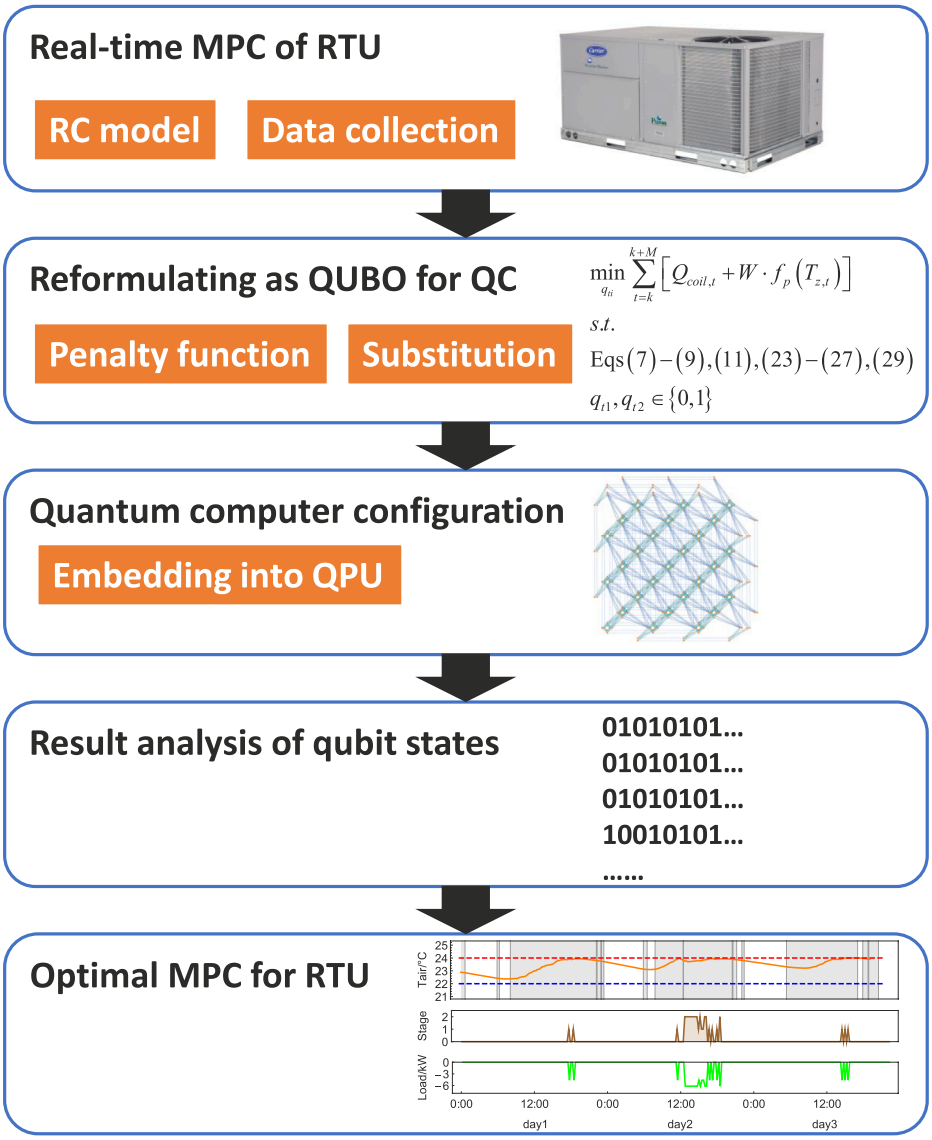

Fig. 1. Overview of the methodology in this study.

written in the following form [82]:

$$\begin{aligned} &\min_{u_0,\ldots,u_{N-1}} \sum_{k=0}^{N-1} \ell_k(x_k, y_k, r_k, u_k, s_k) \\ &s.t. \\ &x_{k+1} = f(x_k, u_k, d_k) \\ &y_k = g(x_k, u_k, d_k) \\ &s_k = h(x_k, y_k, u_k, d_k) \\ &x_0 = \widehat{x} \\ &x_k \in \mathscr{X}, \mathrm{u_k} \in \mathscr{U}, \mathrm{s_k} \in \mathscr{S} \\ &k \in \mathbb{N}_0^{N-1} \end{aligned} \tag{4}$$

Where ℓ_k is the objective function, x_k the system states, y_k the system outputs, r_k the reference signal, u_k the system inputs, s_k the slack variables, d_k the disturbances, x_0 the initial state, $\mathscr{X}$ the constraints for x_k, $\mathscr{U}$ the constraints for u_k, $\mathscr{S}$ the constraints for s_k, k the time step, and N the prediction horizon. The optimal control would minimize the objective function, such as energy use or electricity bill for the building HVAC systems affected by the disturbances and within the constraints of comfort and system bounds.

To solve this optimization problem by quantum computing, we first needed to formulate the constrained problem into an unconstrained one by employing penalty terms in the objective function for x_k, u_k, s_k. Then we needed to formulate the system inputs u_k in the form of binary qubits. Thus, the optimization can be reformulated in the following form:

$$\begin{aligned} &\min_{q_{ki}} \left[\ell_{\mathscr{X}}(x_k) + \ell_{\mathscr{U}}(u_k) + \ell_{\mathscr{S}}(s_k) + \sum_{k=0}^{N-1} \ell_k(x_k, y_k, r_k, u_k, s_k) \right] \\ &s.t. \\ &x_{k+1} = f(x_k, u_k, d_k) \\ &y_k = g(x_k, u_k, d_k) \\ &s_k = h(x_k, y_k, u_k, d_k) \\ &x_0 = \widehat{x} \\ &u_k = u_k(q_{ki}) \\ &k \in \mathbb{N}_0^{N-1} \\ &q_{ki} \in \{0, 1\} \end{aligned} \tag{5}$$

Even the objective function, the state-space model, the system model, and the penalty function were non-linear, as long as $\ell_{\mathscr{X}}, \ell_{\mathscr{U}}, \ell_{\mathscr{S}}, \ell_k, f, g, h, u_k$ were polynomial functions, the above objective function

was a polynomial of q_{ki}. As a result, the form of the objective function was the same as Eq (2). Previously, researchers [83,84] have developed algorithms to convert the problem from PUBO to QUBO - from Eq (2) to Eq (3). Hence, quantum computing could resolve the MPC problem for building HVAC systems. In this paper, we used quantum computing to solve the non-linear mixed-integer programming for RTU optimal control as an example.

3.2. Quantum computing for optimizing RTU operation

Fig. 1 shows the overview of the methodology in this study. We first built the real-time MPC of the RTU in the building with discrete fan stage variables to minimize the total coil load and electricity price across the prediction horizon. We developed the thermal network model and collected the data to calibrate the model. Then, we reformulated the problem as the QUBO by using a penalty function and the substitution method. We could find the coefficients through programming. Then we used the D-Wave advantage, which was a commercial quantum computing equipment. We used Python to submit the coefficients to D-Wave quantum computer by Leap cloud system. By minor embedding the nodes and edge weights of the chimeric graph architecture of qubits, the D-Wave quantum computer could solve such optimization problems and find the global optimum by outputting qubits states of 0/1 from the quantum processor unit (QPU). Therefore, we could analyze the results and obtain the optimal MPC solutions for the RTU fan stages.

3.2.1. MPC and coil load calculation

In this study, the purpose of the MPC for building HVAC systems was to minimize the coil load or electricity price used by an RTU of EcoBlue technology 48GCM04 for cooling in summer, while maintaining the room air temperature around a set point when the room was occupied. When the room was unoccupied, we also applied setback control to save energy. The optimization of the MPC for coil load can be written as

$$\begin{aligned} &\min_{s_t} \sum_{t=k}^{k+M} Q_{coil} \\ &s.t. \\ &\dot{\boldsymbol{X}} = \boldsymbol{AX} + \boldsymbol{Bu} + \boldsymbol{Ew} \\ &22^\circ C \leqslant T_z \leqslant 24^\circ C \ when\ P_z > 0;\ 10^\circ C \leqslant T_z \leqslant 32^\circ C \ when\ P_z = 0 \end{aligned} \tag{6}$$

where s_t was the discrete fan stage to be optimized, k was the first optimization time step, $k + M$ was the last optimization time step, Q_{coil} was the coil load at each time step, $\boldsymbol{X}$ was the state of the building (i.e., wall temperature and zone air temperature), $\boldsymbol{u}$ was the cooling load of the RTU, $\boldsymbol{w}$ was the uncontrollable inputs including ambient air temperature, solar heat gain, and internal heat gains, T_z was the zone air temperature, P_z was the number of occupants. The constraints were that air temperature should be around the set point temperature 23 $^\circ C$ with a dead band of 1$^\circ C$. Setback when unoccupied was 10 $^\circ C$ for the heating season and 32 $^\circ C$ for cooling. The zone air temperatures at future time steps were predicted by the state-space model. For the MPC of building HVAC systems, the control time step was 15 min. In this paper, we used the prediction horizon with 2, 3, 6, 12, and 24 h. Thus, we optimized 8, 12, 24, 48, and 96 time steps in future horizons.

In addition, the electricity price could vary due to the grid demand response. For example, there was difference between the time-of-use energy rate during the peak time and off-peak time. In the summer season when the outdoor air temperature was hot and grid stress was high, the electricity price would be higher. It could reduce the energy usage during the time of high grid stress and emergencies. The optimization of the MPC for electricity price could be written when the objective function in Eq. (6) is $Q_{coil} \cdot price(t)$, and $price(t)$ was the electricity price per kWh. At each time step, we needed to manipulate the system inputs, the stage of fan s_t, with the consideration of several future prediction horizons. Therefore, s_t was a discrete variable with possible values 0, 1, or 2 to be optimized. Here 0 represented fan off status, while 1 and 2 represented stages I and II, respectively. Various stages of the fan represented different powers and speeds. It could be adjusted according to the need and circumstances for load requirement and energy efficiency.

Table 1
Value of coefficients to calculate EIRT and CCMT.

Coefficient	Value	Coefficient	Value
C_0	1.2788	C_6	0.15979
C_1	−0.0019315	C_7	−0.0012132
C_2	−0.000239	C_8	5.4e-5
C_3	−0.066933	C_9	−0.0050051
C_4	0.0010513	C_{10}	0.00025547
C_5	0.00058568	C_{11}	−0.00012701

We evaluated the coil load at each time step using the following equations

$$Q_{coil} = Q_{ref} \cdot EIR \cdot f_{EIRT} \cdot f_{CCMT} \cdot V_{supply} \tag{7}$$

$$f_{EIRT} = C_0 + C_1 T_o + C_2 T_o^2 + C_3 T_{mix} + C_4 T_{mix}^2 + C_5 T_o T_{mix} \tag{8}$$

$$f_{CCMT} = C_6 + C_7 T_o + C_8 T_o^2 + C_9 T_{mix} + C_{10} T_{mix}^2 + C_{11} T_o T_{mix} \tag{9}$$

where the coil load was proportional to a given reference load, a constant energy input ratio (EIR), energy input ratio temperature (EIRT), compressor control module temperature (CCMT), and supply airflow rate V_{supply}. The performance curves of EIRT and CCMT were the non-linear functions of the outdoor air temperature T_o and the mixed air temperature T_{mix}. $C_0 \sim C_{11}$ were coefficients provided by the manufacturer, as Table 1 shows [85]. Thus, the coil load was a quartic polynomial of T_{mix}.

The mixed air temperature in the duct was related to the stage of the fan s_t, the outdoor air flow rate $V_{o,t}$, and the supply air flow rate $V_{supply,t}$ as

$$T_{mix,t} = \begin{cases} T_{o,t}, \text{if } s_t = 0 \\ \left[\dfrac{V_{o,t}}{V_{supply,t}} T_{o,t} + \left(1 - \dfrac{V_{o,t}}{V_{supply,t}}\right) T_{z,t}\right], \text{if } s_t = 1 \text{ or } 2 \end{cases} \tag{10}$$

When the fan was off, the mixed air temperature was the same as the outdoor air temperature. When the fan was on, the mixed air temperature was the volume-weighted average of outdoor air temperature and zone return air temperature.

The required outdoor airflow rate of the RTU was based on the ASHRAE Standard 62.1 [86] as

$$V_{o,t} = \frac{R_p P_{z,t} + R_a A_z}{E_z} \tag{11}$$

where R_p was the outdoor air flow rate required per person, $P_{z,t}$ the zone population, R_a the outdoor airflow rate required per unit area, A_z the zone floor area, E_z the zone air distribution effectiveness. In this study, we used $R_p = 8.5 \text{m}^3/\text{h}$ per person, $R_a = 1.1 \text{m}^3/\text{h}$, $A_z = 68 \text{m}^2$, and $E_z = 1$ according to ASHRAE Standard 62.1 [86].

The supply airflow rate of the RTU at each time step was related to s_t, so that

$$V_{supply,t} = \begin{cases} 0, s_t = 0 \\ V_1, s_t = 1 \\ V_2, s_t = 2 \end{cases} \tag{12}$$

Where $V_1 = 0.32 \text{m}^3/\text{s}$ (675 CFM) and $V_2 = 0.42 \text{m}^3/\text{s}$ (900 CFM), which were provided by the manufacturer.

We still needed to predict the zone air temperature at upcoming time steps for the predictive control, which would be introduced in the next subsection. With Eqs (7) - (12), we could calculate the coil energy use, whose total in the next several time steps would be minimized by MPC. It was worthy to note that for each additional optimization time step, the

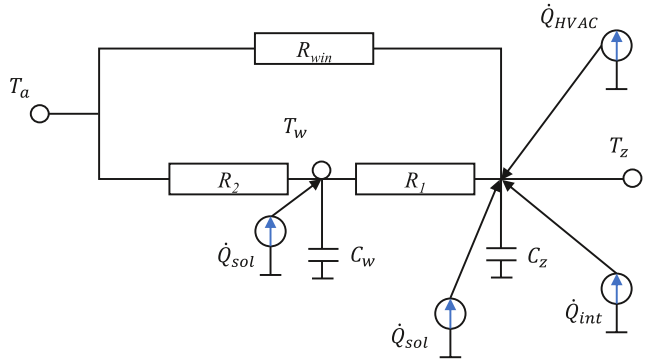

Fig. 2. RC network model for the room equipped with RTU.

number of possible combinations of system inputs tripled. As a result, when the number of prediction horizons and solution space was large, it was extremely difficult to find the optimum control quickly by traditional optimization methods. For coordinated control of several RTUs [31,87] and large-scale MPC problems [88], the optimization would be more difficult.

3.2.2. RC model for room air temperature

Fig. 2 shows a thermal resistance–capacitance (RC) network model to predict the zone air temperature for the MPC. The governing equations of the state-space model for the wall temperature and zone air temperature were

$$\dot{T}_w = \frac{T_a - T_w}{C_w R_2} + \frac{T_z - T_w}{C_w R_1} + \frac{\dot{Q}_{sol}}{C_w} \tag{13}$$

$$\dot{T}_z = \frac{T_w - T_z}{C_z R_1} + \frac{T_a - T_z}{C_z R_{win}} + \frac{\dot{Q}_{HVAC} + \dot{Q}_{int} + \dot{Q}_{sol}}{C_z} \tag{14}$$

Where T_a was the ambient air temperature, T_w the wall temperature, T_z the zone air temperature, $\dot{Q}_{sol}$ the heat gain from solar radiation on walls and the air node, $\dot{Q}_{HVAC}$ the heat gain from the HVAC system, $\dot{Q}_{int}$ the heat gains from internal sources, R_{win} the window thermal resistance, R_1 and R_2 the thermal resistance of the exterior wall, C_w the exterior wall heat capacity, and C_z the zone heat capacity.

We could write Eqs (13)-(14) in matrix form as

$$\dot{\boldsymbol{X}} = \boldsymbol{A}\boldsymbol{X} + \boldsymbol{B}\boldsymbol{u} + \boldsymbol{E}\boldsymbol{w} \tag{15}$$

$$\boldsymbol{X} = [T_w \quad T_z]^T \tag{16}$$

$$\boldsymbol{A} = \begin{bmatrix} -\frac{R_1 + R_2}{C_w R_1 R_2} & \frac{1}{C_w R_1} \\ \frac{1}{C_z R_1} & -\frac{R_1 + R_{win}}{C_z R_1 R_{win}} \end{bmatrix} \tag{17}$$

$$\boldsymbol{B} = \begin{bmatrix} 0 & \frac{1}{C_z} \end{bmatrix}^T \tag{18}$$

$$\boldsymbol{u} = \dot{Q}_{HVAC} \tag{19}$$

$$\boldsymbol{E} = \begin{bmatrix} \frac{1}{C_z R_2} & \frac{1}{C_w} & 0 \\ \frac{1}{C_z R_{win}} & \frac{1}{C_z} & \frac{1}{C_z} \end{bmatrix} \tag{20}$$

$$\boldsymbol{w} = \begin{bmatrix} T_{amb} & \dot{Q}_{sol} & \dot{Q}_{int} \end{bmatrix}^T \tag{21}$$

The heat gain from the HVAC systems was calculated as

$$\dot{Q}_{HVAC} = c_{air}\rho_{air}V_{supply}(T_{supply} - T_z) \tag{22}$$

We used T_{supply} with 12°C for cooling the room in this study. For the other parameters of thermal resistance and heat capacity, we used the collected data in the office to calibrate the values of these parameters.

The discretized state-space model of Eq (15) was

$$\boldsymbol{X}_t = e^{\boldsymbol{A}T}\boldsymbol{X}_{t-1} + \boldsymbol{A}^{-1}(e^{\boldsymbol{A}T} - \boldsymbol{I})\boldsymbol{B}\boldsymbol{u}_{t-1} + \boldsymbol{A}^{-1}(e^{\boldsymbol{A}T} - \boldsymbol{I})\boldsymbol{E}\boldsymbol{w}_{t-1} \tag{23}$$

Where **I** was the identity matrix.

Thus, the solution of the above discretized state-space RC model could be written as

$$\begin{bmatrix} T_{w,t} \\ T_{z,t} \end{bmatrix} = e^{\boldsymbol{A}T(t-1)}\begin{bmatrix} T_{w,1} \\ T_{z,1} \end{bmatrix} + \sum_{i=1}^{t-1} e^{\boldsymbol{A}T(t-1-i)}\boldsymbol{A}^{-1}(e^{\boldsymbol{A}T} - \boldsymbol{I})\boldsymbol{B}\boldsymbol{u}_i + \sum_{i=1}^{t-1} e^{\boldsymbol{A}T(t-1-i)}\boldsymbol{A}^{-1}(e^{\boldsymbol{A}T} - \boldsymbol{I})\boldsymbol{E}\boldsymbol{w}_i \tag{24}$$

3.2.3. Data collection

We collected all the data in an office building on the campus of Syracuse University, as shown in Fig. 3. Fig. 4 also shows the data collection devices. Fig. 4 (a) demonstrates that we used a people

(a) (b)

Fig. 3. Photos of the building and the office room for data collection.

Fig. 4. Data collection devices in this study: (a) sensor (Density Entry) for measuring the number of occupants in the room; (b) sensor for measuring supply air temperature and on the diffuser.

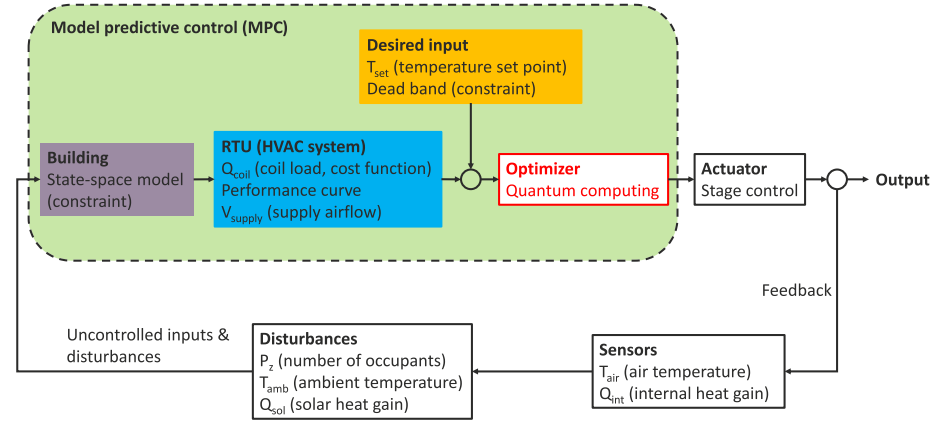

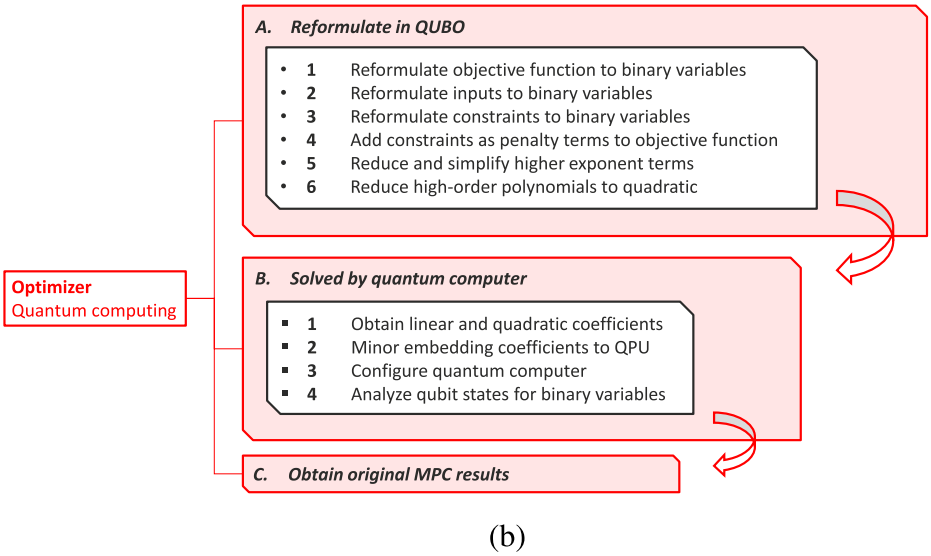

Fig. 5. (a) MPC block diagram using quantum computing. (b) Process of formulating the HVAC control problem to QUBO and solved by quantum computing.

counting sensor (Density Entry) to collect the room occupancy data. It used the depth sensor and infrared lasers to measure the entry movement. There were air temperature sensors, flow rate sensors, and smart meters equipped in the room. So we could also monitor the zone air temperature, internal heat gain, supply air temperature, and supply air flow rate of the HVAC system by using installed sensor (HOBO data

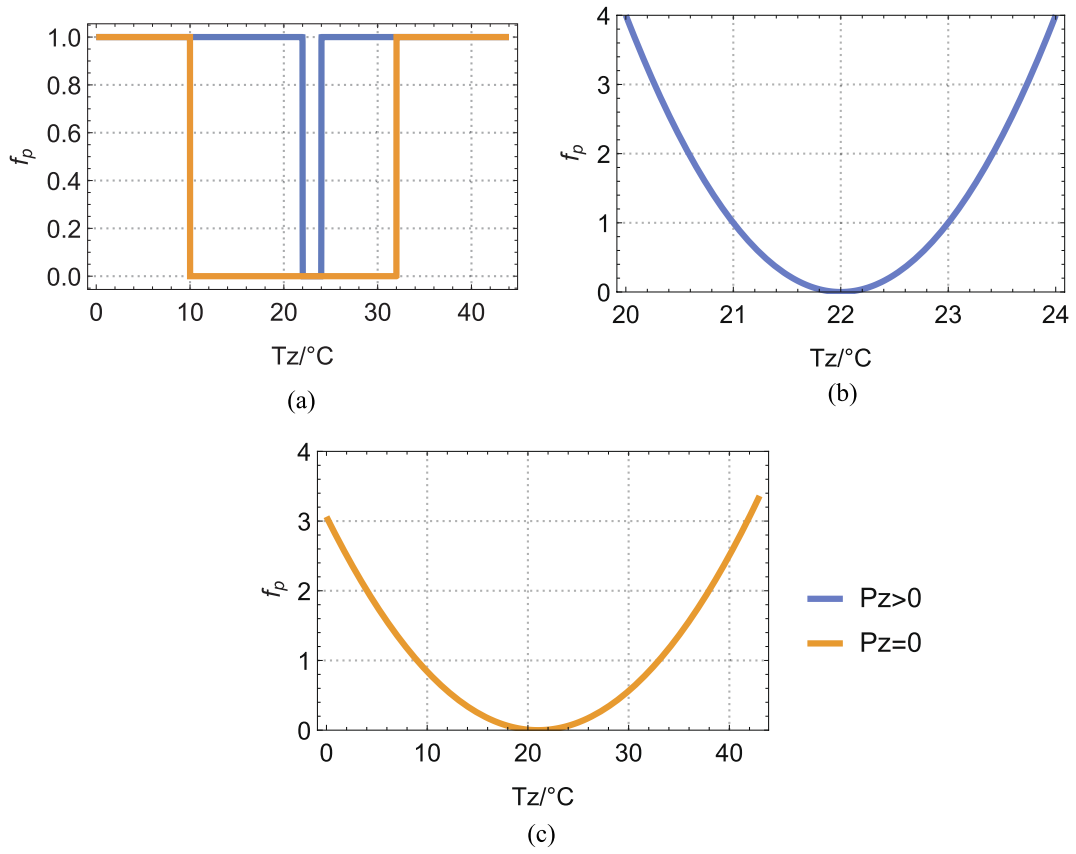

Fig. 6. (a) Ideal penalty functions; (b) penalty function we used when the room was occupied; and (c) penalty function we used when the room was unoccupied.

logger MX1102A, temperature measurement range and accuracy: 0° to 50 °C and ± 0.21 °C from 0° to 50 °C) and Building Automation and Control Networks (BACnet) [89]. We programmed it in Python and the data were automatically read and placed in the PostgreSQL database. As for the outdoor weather information, we used the data from the Syracuse STEM weather station. The internal heat gain, outdoor weather data, and room occupancy data were also used in MPC as disturbances. We collected data for three days in the summer season of 2021 and the frequency of data collection was 5 min.

3.3. Binary optimization for quantum computing

Fig. 5 shows the MPC block diagram using quantum computing and the process of formulating the HVAC control problem to QUBO for quantum computing. For the MPC optimization of the RTU, the objective function in Eq (6) was for constrained optimization with discrete variabless_t. We needed to reformulate the constrained optimization problem to an unconstrained binary optimization so that it could become a PUBO as Eq (2), and further formulate it into QUBO as Eq (3) for quantum computing.

At first, the supply air flow rate and mixed air temperature in Eq (10) and (12) could be written in a unified form instead of the piecewise form as

$$T_{mix,t} = \frac{(s_t-1)(s_t-2)}{2}T_{o,t} - s_t(s_t-2)\left[\frac{V_{o,t}}{V_1}T_{o,t} + \left(1 - \frac{V_{o,t}}{V_1}\right)T_{z,t}\right] + \frac{s_t(s_t-1)}{2}\left[\frac{V_{o,t}}{V_2}T_{o,t} + \left(1-\frac{V_{o,t}}{V_2}\right)T_{z,t}\right] \quad (25)$$

$$V_{supply,t} = \frac{s_t(s_t-1)}{2}V_2 - s_t(s_t-2)V_1 \quad (26)$$

Thus, V_{supply} and T_{mix} were quadratic polynomials of s_t.

Then with the thermal network model, we could calculate the predicted state of zone air temperature and wall temperature at any time step by using Eq (24). The first and last terms were given constant at each time step, and V_{supply} in the second term was a quadratic polynomial of s_t. So $T_{z,t}$ was also a quadratic polynomial of s_t.

Next, there were constraints of zone air temperature in Eq (6). In this study, we used a penalty function adding to the objective function to convert the constrained optimization to unconstrained optimization. The ideal penalty function was step functions as shown in Fig. 6(a). Since we could only use polynomial optimization for quantum computing, we used quadratic penalty functions when the room was occupied and unoccupied. Fig. 6(b) and (c) show the penalty functions that

$$f_p = \begin{cases} (T_z - 23)^2, P_z > 0 \\ \left(\frac{T_z - 21}{12}\right)^2, P_z = 0 \end{cases} \quad (27)$$

Therefore the new objective function could be written as

$$\min_{s_t} \sum_{t=k}^{k+M} \left[Q_{coil,t} + W \cdot f_p(T_{z,t})\right] \quad (28)$$

where W was a weight to control the importance between the coil load and the penalty of air temperature deviation. Large weight could increase the impact of deviations from the temperature set point. And $f_p(T_{z,t})$ was a quadratic polynomial of s_t.

Since the optimized stage of the fan in each time step $s_t \in \{0,1,2\}$, we used two binary variables $q_{t1}, q_{t2} \in \{0,1\}$ to represent as

$$s_t = q_{t1} + q_{t2} \quad (29)$$

In particular, for the fan stage to be optimized at the next time step in the prediction horizon, it was represented by the first two qubits.

Hence, we could finally formulate the optimization of MPC into a

binary optimization for any time step k as

$$\begin{aligned}&\min_{q_{ti}} \sum_{t=k}^{k+M}\left[Q_{coil,t}+W\cdot f_p\left(T_{z,t}\right)\right]\\&s.t.\\&\text{Eqs}(7)-(9),(11),(23)-(27),(29)\\&q_{t1},q_{t2}\in\{0,1\}\end{aligned} \tag{30}$$

We found that the objective function in above optimization problem was a tenth-degree polynomial of the binary variablesq_{ti}. Note that

$$q_i^n=q_i \tag{31}$$

when $q_i\in\{0,1\}$ and n was a positive integer. The higher exponent terms could be further simplified and reduced to one.

After a simplification, we found that the objective function contained not only linear and non-linear second-order terms, but also three-order and four-order terms, as the following form:

$$H=\sum_i C_i q_i+\sum_{i,j} C_{ij}q_iq_j+\sum_{i,j,k} C_{ijk}q_iq_jq_k+\sum_{i,j,k,l} C_{ijkl}q_iq_jq_kq_l \tag{32}$$

Note that the constant term did not affect the optimization result, thus it was removed.

Then we also needed to reduce the high-order polynomials of objective function from four-order PUBO as Eq (2) into QUBO as Eq (3). Based on the Handbook of D-Wave quantum annealer [90] and literatures [83,84], the non-quadratic polynomials could be reformulated and reduced to quadratics by minimum selection method [83] and substitution method [84].

Minimum selection method worked on only one term, by introducing an ancillary binary variable w, to minimize a cubic term of $C_{ijk}q_iq_jq_k$

$$\begin{aligned}&\min C_{ijk}q_iq_jq_k\\&s.t.q_i,q_j,q_k\in\{0,1\}\\&\Leftrightarrow\begin{cases}\min C_{ijk}w\left(q_i+q_j+q_k-2\right),C_{ijk}<0\\\min C_{ijk}\left[(w-1)\left(q_i+q_j+q_k-1\right)+q_iq_j+q_iq_k+q_jq_k\right],C_{ijk}>0\end{cases}\end{aligned} \tag{33}$$

Similarly, for minimization of a quartic term $C_{ijkl}q_iq_jq_kq_l$

$$\begin{aligned}&\min C_{ijkl}q_iq_jq_kq_l\\&s.t.q_i,q_j,q_k,q_l\in\{0,1\}\\&\Leftrightarrow\begin{cases}\min C_{ijkl}w\left(q_i+q_j+q_k+q_l-3\right),C_{ijkl}<0\\\min C_{ijkl}\left\{w\left[-2\left(q_i+q_j+q_k+q_l\right)+3\right]+q_iq_j+q_iq_k+q_iq_l+q_jq_k+q_jq_l+q_kq_l\right\},C_{ijkl}>0\end{cases}\end{aligned} \tag{34}$$

Since there was more than one high-order term in the objective function in Eq (32) of this study, we also used the substitution method [84]. The algorithm was as follows: as long as there existed high-order terms containing q_iq_j like $C_{ijk}q_iq_jq_k$ or $C_{ijkl}q_iq_jq_kq_l$ in the polynomial of objective function H, we introduced an ancillary binary variable w_{ij} to replace q_iq_j and looped through the operations as follows:

$$C_{ij}q_iq_j=C_{ij}w_{ij} \tag{35}$$

$$C_{ijk}q_iq_jq_k=C_{ijk}w_{ij}q_k \tag{36}$$

$$C_{ijkl}q_iq_jq_kq_l=C_{ijk}w_{ij}q_kq_l \tag{37}$$

$$H=H+M\left[q_iq_j-2\left(q_i+q_j\right)w_{ij}+3w_{ij}\right] \tag{38}$$

Where H was the polynomial of objective function in Eq (32), and M [84] was defined as

$$M\triangleq 1+\sum_{ij}\left|C_{ij}\right| \tag{39}$$

The above Eq (38) was established since the minimum of H has not changed as the following two equivalences [84] for any $q_i,q_j,w_{ij}\in\{0,1\}$ always hold

$$q_iq_j=w_{ij}\Leftrightarrow q_iq_j-2\left(q_i+q_j\right)w_{ij}+3w_{ij}=0 \tag{40}$$

$$q_iq_j\neq w_{ij}\Leftrightarrow q_iq_j-2\left(q_i+q_j\right)w_{ij}+3w_{ij}>0 \tag{41}$$

From the aforementioned Eqs (35)-(38), the four-order PUBO as Eq (32) can be gradually reduced to QUBO. Similarly, the interaction of more than four variables could also be reduced by sequentially introducing new binary variables, but they did not appear in the objective function of this study. Finally, the problem could be written as QUBO in the form of Eq (3). And it could be mapped and solved by the D-Wave quantum computer.

3.4. D-Wave annealer configuration

After reformulating the problem as the QUBO, we obtained the linear coefficients and non-linear quadratic coefficients. The minor embedding would map them to the nodes and edge weights of the chimeric graph architecture of qubits in the QPU. With these qubit biases and coupling strengths on the D-Wave quantum computer, it could use quantum annealing to minimize the Hamiltonian energy of this configuration. Therefore, the system could find the lowest energy state of this configuration, which corresponded to the global minimum of the objective function with high probability [91].

In order to find the optimal solutions to the QUBO problems, we used the D-Wave advantage, which was a commercial quantum computing equipment aiming to achieve quantum annealing. The D-Wave Advantage system contained a QPU with over 5000 qubits and 35,000 couples among qubits [92]. The QPU needed to operate at a temperature of 12 mK and be isolated from the surrounding environment. The topology structure of the QPU was Pegasus as shown in Fig. 1, with the graph size of P16 and connectivity of Degree 15. After the quantum computer reached the low energy solution of the Hamiltonian after annealing as Eq (1), it could output the samples of states of the qubits. As a result, we were able to obtain the corresponding optimal solution of the QUBO and the original optimization problem for the RTU. The time of one annealing process on D-Wave Advantage was 2 μs. In order to obtain a reasonable optimal solution, we used the number of reads with 10,000 times for the annealing process. We used Python to submit the coefficients of the QUBO to D-Wave annealer by Leap cloud system [93].

3.5. Comparison with other control strategies and traditional optimization method

3.5.1. Baseline control strategy

To verify the results of the MPC by quantum computing, we evaluated the energy savings of the MPC and compared it with other control

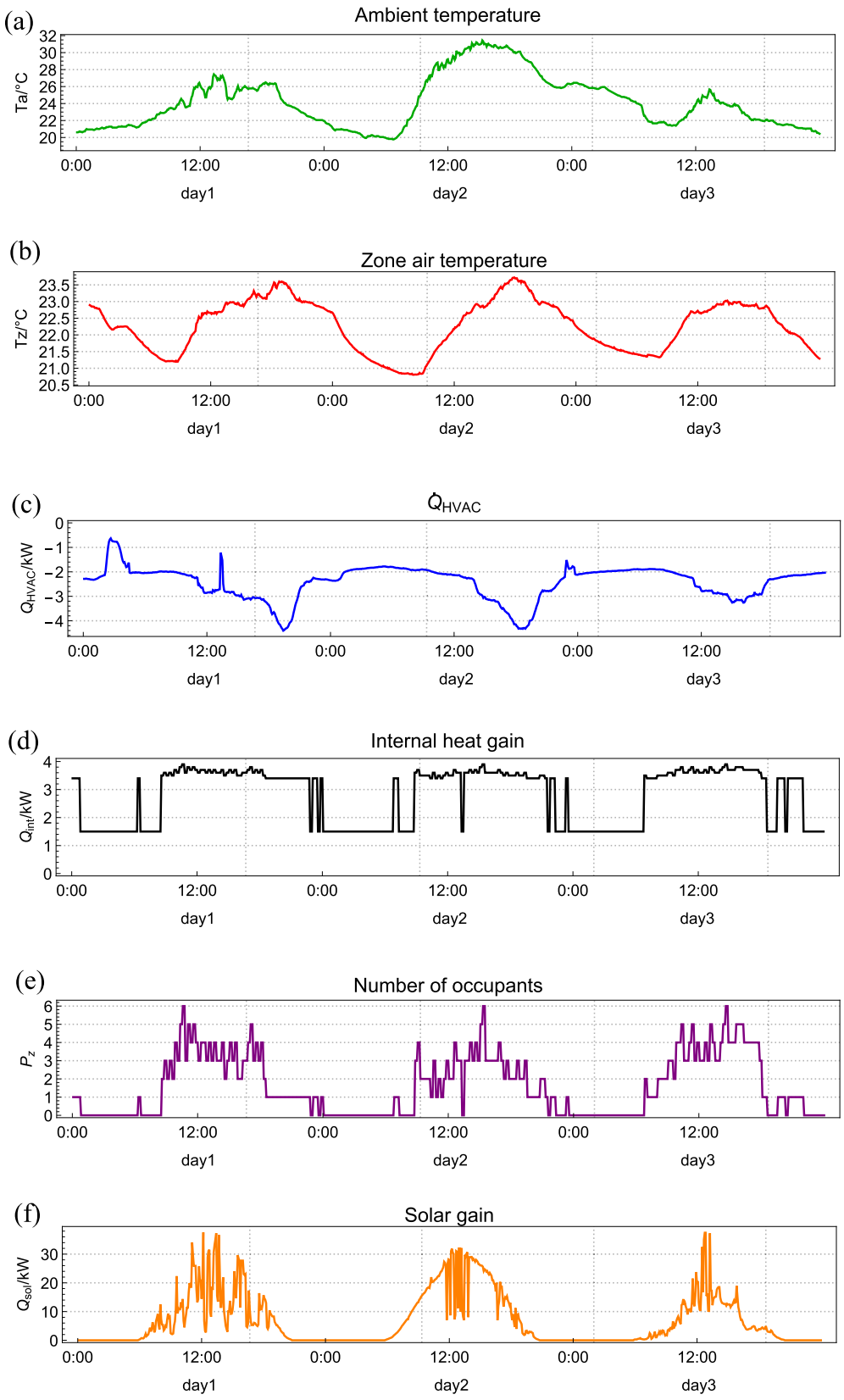

Fig. 7. Collected data of (a) ambient air temperature; (b) zone air temperature; (c) cooling load by HVAC system; (d) internal heat gain; (e) number of occupants; (f) solar heat gain.

Table 2
Raw outputs of quantum computing at 20th time step.

Sample	q1	q2	q3	q4	q5	…	Hamiltonian
1	0	0	0	0	0	…	5.246113e-3
2	0	0	1	0	0	…	6.526900e-3
3	0	0	0	0	0	…	6.535851e-3
4	0	0	0	0	0	…	6.535851e-3
5	0	0	0	0	0	…	7.294013e-3
6	0	0	0	0	0	…	7.295246e-3
7	0	0	0	0	0	…	7.522984e-3
8	0	0	0	0	0	…	7.962238e-3
9	0	0	0	0	0	…	7.973845e-3
10	0	0	0	0	0	…	8.037716e-3
…	…	…	…	…	…	…	…

strategies. In this study, we compared with fixed rule-based on–off control coupling the setback control with ASHRAE Guideline 36 [94]. For on–off control, the temperature set point was always equaled the occupied set point of 23°C. For setback control, the set point in occupied time was the same. In the unoccupied time before 8:00 and after 17:30, the set point was 32°C. The control algorithm at each time step was as follows:

- If zone air temperature was higher than the set point, and fan stage was off ⟶ fan stage I.
- If zone air temperature was higher than the set point and the one at the previous time step, and fan stage I was on ⟶ fan stage II.
- If zone air temperature was lower than the set point and fan stage II was on ⟶ fan stage I.
- If zone temperature was lower than the set point and cooling stage I was on ⟶ fan stage off.
- Otherwise ⟶ keep the current fan stage.

3.5.2. Traditional optimization method

To validate the feasibility and efficiency of quantum computing for MPC of building HVAC systems, we also compared the computing time with traditional optimization methods. We solved the non-linear discrete optimization of MPC as Eq (30) by using GA in the Global Optimization Toolbox in MATLAB R2021a. It was a popular algorithm that mimic a natural selection process that repeatedly modified a population of individual solutions that were restricted to integral values. In order to obtain reasonable results, the population size was based on the number of binary variables to be optimized. We set the max stall generations with 50, and optimization function tolerance with 1e-4.

In addition, we also solved the QUBO as Eq (30) by using Gurobi 9.0.1. It used the cutting plane algorithm to find the optimized results for the mixed-integer quadratic programming. We set the optimal solution tolerance with 1e-4.

4. Results

4.1. Collected data

Fig. 7 shows the collected data on ambient air temperature, zone air temperature,$\dot{Q}_{HVAC}$, number of occupants, $\dot{Q}_{int}$ and $\dot{Q}_{sol}$ on three days in summer. The data were collected between July 14th-16th, 2021. For internal heat gains, they contained heat from occupants, light bulbs, and internal appliances. Based on the actual information about the room, we assumed that the heat gain was 100 W per occupant, 60 W per bulb, 100 W per desktop, and 30 W per monitor [95]. When the room was occupied, all the lights were on. And the number of working desktops was the same as number of occupants. We used these data to calibrate the RC model and obtained the values of the parameters, as listed in Table A1. The calibrated RC model could predict the room air temperature with root mean square error of less than 0.2°C. So the model can be used to predict the room thermodynamics. We also used the ambient air temperature, the number of occupants in the room, solar heat gain, and the internal heat gain for the MPC as disturbances.

4.2. Results of quantum computing

After the reformulation, we were able to obtain all the linear and quadratic coefficients of QUBO for quantum computing. We got 10,000

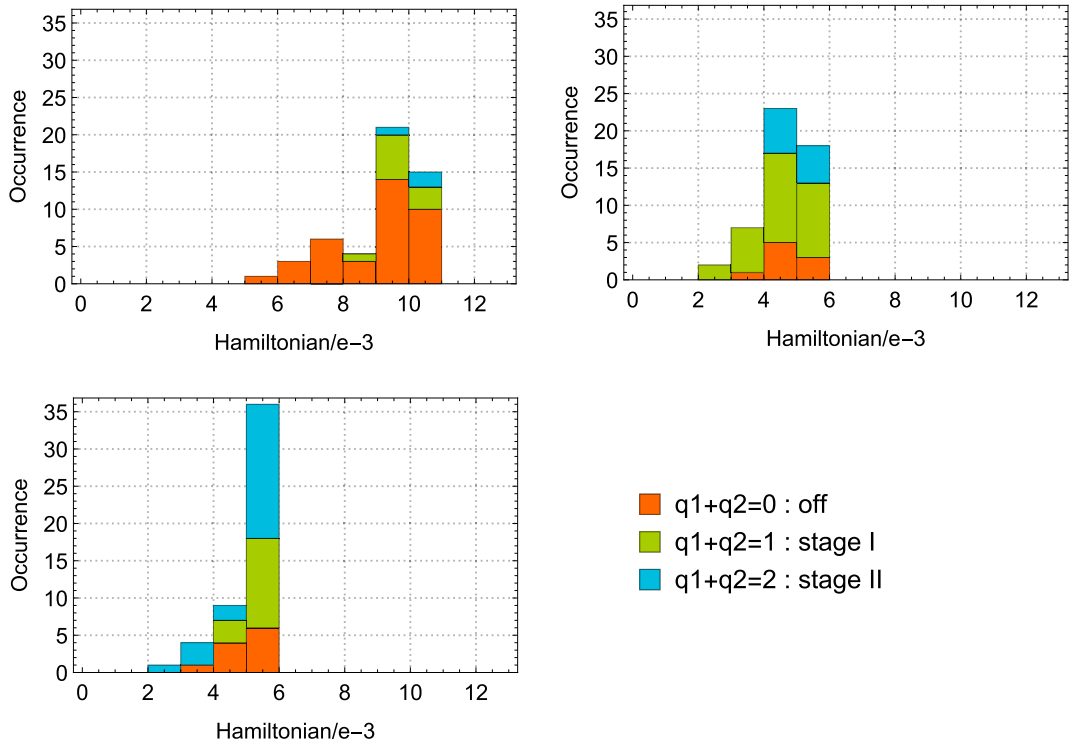

Fig. 8. Hamiltonian distribution of 50 smallest samples at (a) 20th, (b) 70th, and (c) 143rd time steps.

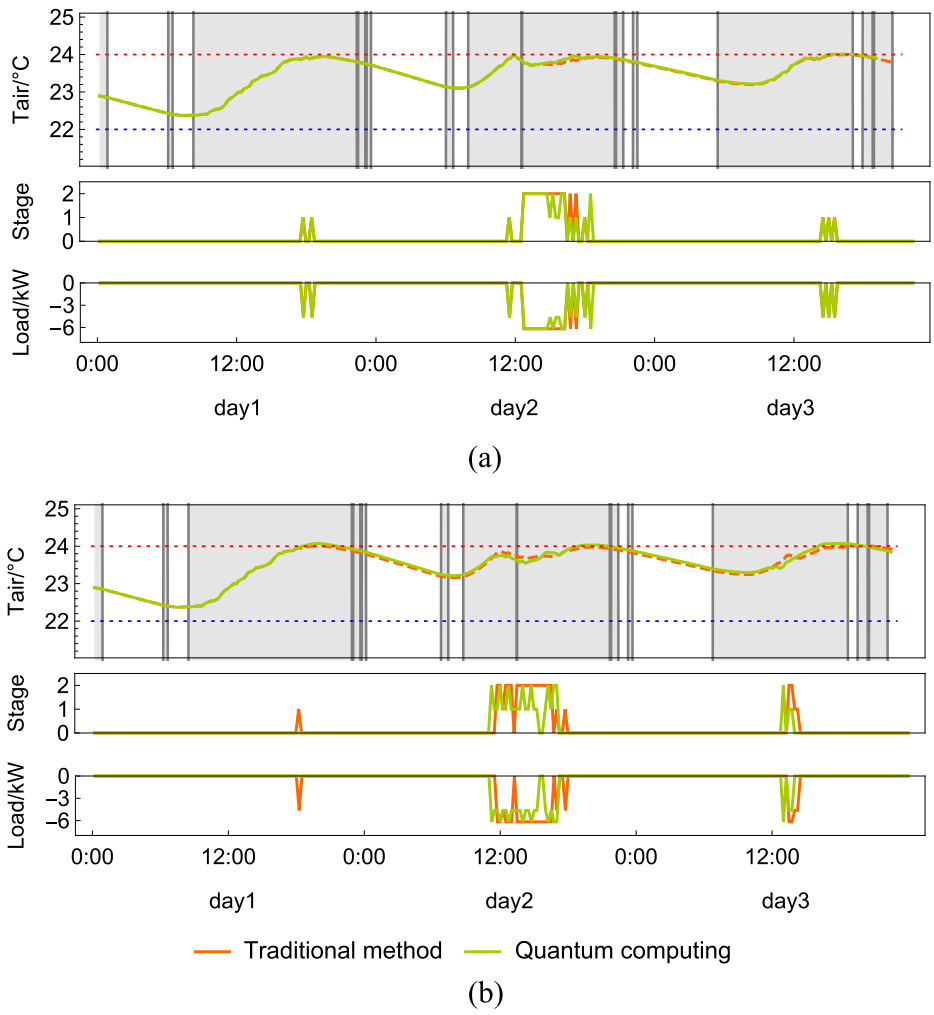

Fig. 9. Comparison of optimal air temperature control, fan stage, and cooling load between quantum computing and traditional optimization method for (a) 2-hour prediction horizon; (b) 3-hour prediction horizon. And gray shade represents the room was occupied.

annealing samples in each time step that could acquire stable results with a high probability of reaching the global minimum. Table 2 lists the raw outputs of quantum computing at the 20th time step for a 3-hour prediction horizon. This table lists ten sample results in the order of Hamiltonian as Eq (1) from small to large, which was a very small fraction of all output results due to space. For each Hamiltonian energy, the corresponding states of first 5 qubits were listed in the table. We found that q1 + q2 with small Hamiltonian had a high probability of being equal to 0 at the 20th time step. As Eq (29) expressed, these results implied the optimal control of the fan stage at the 20th time step should be 0 and turn off with a high probability.

Fig. 8 shows the occurrence distribution of 50 samples with the lowest Hamiltonian at the 20th, 70th, and 143rd time steps. As low Hamiltonian represented a high probability of global minimum, in these three time steps, the optimal controls were off, stage I and stage II, respectively. Similar to Table 2 and Fig. 8, then we analyzed the outputs to obtain the MPC optimization results at each time step. Therefore, the non-linear optimal control problem of building HVAC system with discrete variables could be resolved by quantum computing.

4.3. Comparison of results and computing time with traditional optimization and control

We got 10,000 annealing samples at each time step that could obtain stable results with a high probability of reaching the global minimum. Then we could analyze the results of quantum annealing at each time step to obtain the optimal control of the RTU fan stage. Fig. 9 compares the optimal air temperature control, fan stage, and cooling load between quantum computing and traditional optimization methods for 2-hour and 3-hour prediction horizons. We found that the RTU used the most cooling load on the second day. In the afternoon when the outdoor air temperature and solar gain were high, the RTU started to cool down the room. After the working hour and at night, the RTU did not work to save energy. We found that the difference in optimal control results between quantum computing and the traditional optimization method occurred in a total of 6 time steps, which was 2.1 % over three days. The predicted cooling load by quantum computing was 1.1 % more than the traditional method. This result showed that quantum computing could obtain optimization results similar to the traditional optimization method. Fig. 9 also shows the predicted air temperature could be controlled within the lower and upper bound of the set point as thermal comfort level by quantum computing. Fig. 10 compares the results of optimal air temperature control, fan stage, and cooling load for quantum computing MPC with 6-hour, 12-hour, and 24-hour prediction horizons. Although most of the cooling load was still used on the second day, the total cooling load did not vary significantly with different prediction horizons. The difference between 6-hour and 24-hour prediction horizon was 6.5 %. Traditional optimization methods were very hard to achieve these results for long prediction horizons.

Fixed on–off control with occupancy information was still used for many buildings. Compared with this baseline control, we found that MPC optimized by the traditional optimization method could save

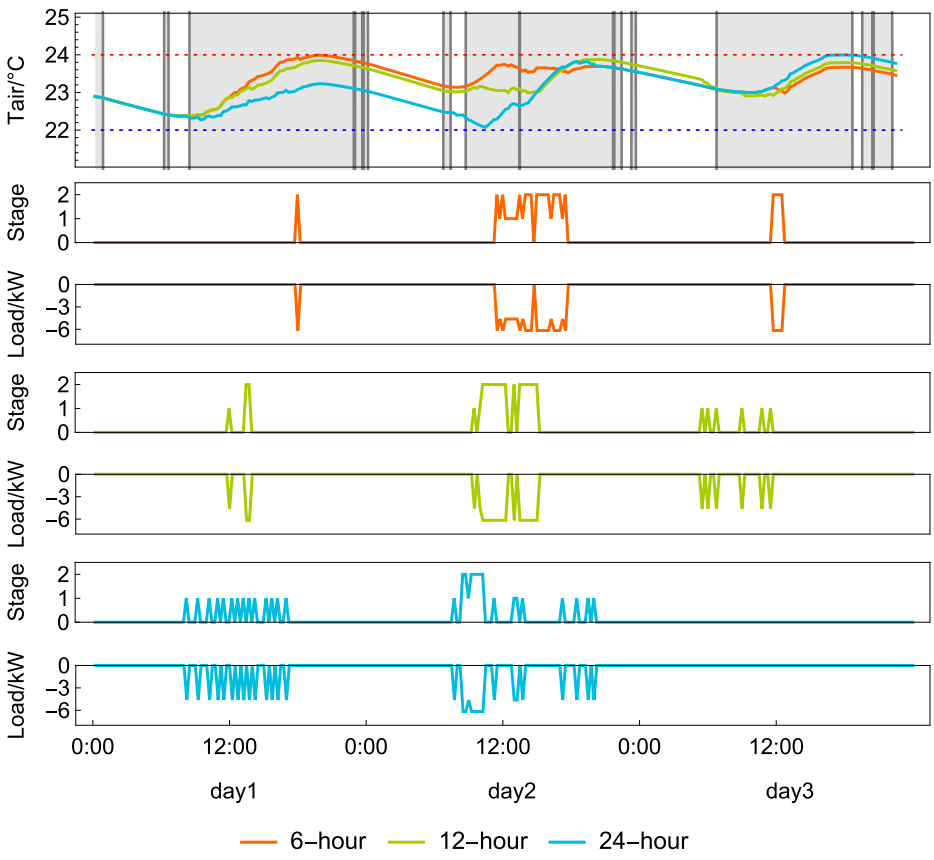

Fig. 10. Comparison of optimal air temperature control, fan stage and cooling load for quantum computing between MPC with 6-hour, 12-hour, and 24-hour prediction horizons. And gray shade represents the room was occupied.

Table 3
Comparison of computing time between quantum computing (QC) and traditional optimization methods.

Prediction horizon	Number of time steps	Number of discrete stages	Number of binary variables	Number of non-linear quadratic terms	Computing time for each time step		
					GA	Gurobi	QC
2 h	8	24	72	237	8 s	0.4 s	1 s
3 h	12	36	159	777	21 s	36 s	1 s
6 h	24	72	577	5430	207 s	greater than4h	1 s
12 h	48	144	2305	22,938	26 min	greater than12 h	6 s
24 h	96	288	9217	94,405	greater than12 h	–	37 s

cooling load by 43.5 %. MPC optimized by quantum computing could save 42.9 % of cooling load. The energy-saving by quantum computing and the traditional optimization method was similar. Hence, we could use quantum computing to optimize the MPC of building HVAC systems the same as the traditional optimization method.

As for the computing time, adding the sampling time, readout time and delay time for the quantum computer, the total QPU time for one

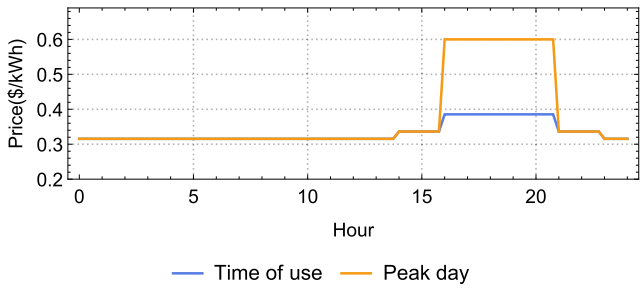

Fig. 11. Electricity price for time-of-use rate and peak day rate in one day.

time step optimization was less than 1 s when the prediction horizon was no more than 6 h. It was almost the same for various prediction horizons and the number of binary variables. That was due to the fact that the quantum annealing and sampling could be operated for all the qubits on QPU simultaneously, making it a truly parallelized calculation [96,97]. In this case, raising the prediction horizon or the number of optimizing variables would not significantly increase the computing time of quantum computing. This phenomenon has also been observed in some previous studies [70]. When the prediction horizon was 12 h, there were more than 2000 binary variables and 20,000 non-linear terms. The quadratic matrix was not sparse and the problem could not be directly embedded in the QPU architecture. The quantum computer needed to use the decomposer to divide the optimization problem into sub-problems to solve. This required some iterative algorithms. Thus, the quantum computing time for 12 h and 24 h prediction horizons was 6 s and 37 s, respectively. Even yet, such computing time was still much shorter than the control time step with 15 min. Hence, quantum computing could respond quickly for larger problems and achieve real-time optimization.

We also carried out the MPC of RTU optimization for larger

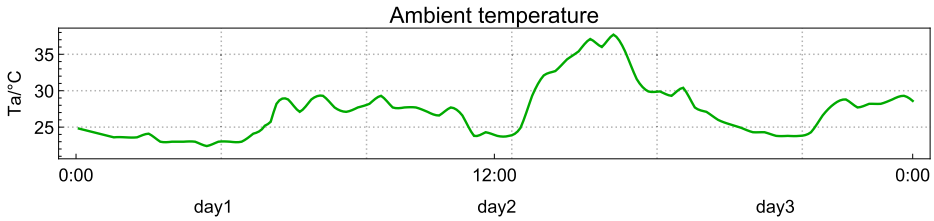

Fig. 12. Ambient air temperature in summer for peak day rate in Los Angeles.

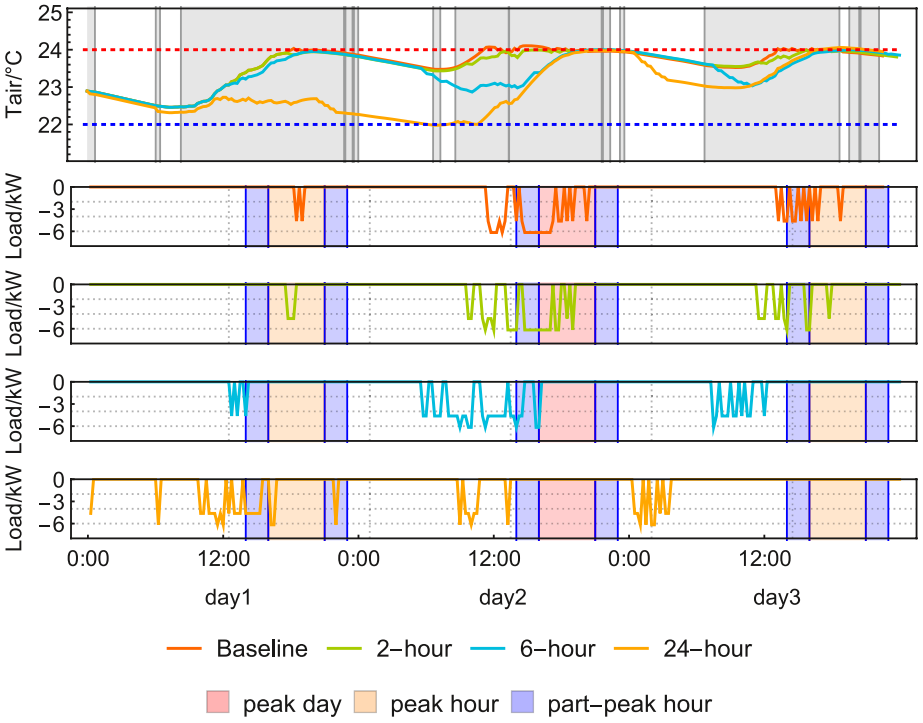

Fig. 13. Comparison of optimal air temperature control and cooling load by quantum computing to minimize the electricity bill between the prediction horizon of 2 h, 6 h, and 24 h and rule-based on/off control as a baseline. The red, orange, and blue shades represent the peak day, peak hour, and part-peak hour, respectively.

prediction horizons by traditional optimization methods. For GA, it could find the optimal solution quickly when the number of binary variables was 72 and 159 in 2 h and 3 h prediction horizons, respectively. However, Table 3 shows that the computing time for each time step was 26 min and over 12 h when the prediction horizon was 12 h and 24 h, respectively. That was due to the huge number of both binary optimized variables and non-linear terms. The program took a longer time to run and obtain a converged result. Similarly, as for Gurobi, it took 36 s to solve the optimization problem with 159 binary variables. However, when there were 577 and 2305 binary variables in the non-linear quadratic optimization problem, it was unable to solve the problem within 4 h and 12 h. Therefore, only quantum computing could achieve real-time optimization if the prediction horizon was more than 12 h. The computing time of quantum computing for solving the quadratic optimization in this study was greatly reduced to less than 0.4 % of that by traditional optimization methods. Increasing the prediction horizon and number of optimizing variables would significantly increase the time of optimization calculation for traditional optimization methods. The problem with more discrete optimization variables could take the advantage of quantum computing. Therefore, quantum computing had greater potential for large-scale optimization problems and even NP-hard problems.

Table 4
Total electricity bills and peak usage calculated by baseline control and quantum computing with various prediction horizons.

Prediction horizon	Total electricity bill/ $	Electricity bill reduction	Peak load/ kWh	Peak load reduction
Baseline control	20.63	–	33.90	–
2 h	20.51	−0.6 %	28.89	−15 %
3 h	19.07	−7.5 %	21.96	−35 %
6 h	18.02	−13 %	5.39	−84 %
12 h	17.12	−17 %	1.54	−95 %
24 h	16.31	−21 %	7.02	−79 %

4.4. Optimization of electricity usage and bill

To reduce the load and the electricity price during peak times, we also used MPC to optimize the fan stage of the RTU. Fig. 11 shows the electricity price for the time-of-use rate and peak day rate [98]. The time-of-use rate for peak, part-peak, and off-peak hours on normal days was $0.38551, $0.33628, and $0.31547 per kWh, respectively. In summer, the peak time was 4 pm to 9 pm, and part-peak time was 2 pm to 4 pm and 9 pm to 11 pm. As for the peak hour on the peak day, the trigger ambient temperature was around 36.7 °C (98°F). The electricity price for the peak hour on the peak day was $0.6 per kWh. The

participants would be notified one day prior to the peak day occurred to respond to the grid signal and arrange the electricity usage to reduce the load. Therefore, to optimize the operation of the RTU for the peak day, we used the actual outdoor air temperature during Sep. 5th-7th 2020 in summer in Los Angeles, California, as Fig. 12 shows. On Sep. 6th during the peak day, the highest air temperature was about 37 °C in the afternoon.

Fig. 13 shows the optimal air temperature control and cooling load using quantum computing for low electricity prices with different prediction horizons and rule-based on/off control as a baseline. The cooling load could be rescheduled to part-peak and off-peak hours by MPC. Especially for 12 h and 24 h ahead prediction horizon, the entire cooling load was not in the peak day. Table 4 lists the electricity bills calculated by quantum computing for 2 h, 3 h, 6 h, 12 h, and 24 h prediction horizons. By using quantum computing, the total electricity bill could be reduced by 21 % compared with the baseline ruled-based on–off control. Regarding the peak hour reduction, Fig. 13 also shows that most of the electrical load was on the peak day and peak hours under baseline control. However, for MPC, 12 h and 24 h prediction control greatly reduced the load in the peak hour and peak day. Table 4 shows that the peak load reduction could be 95 % and 79 % compared with baseline control for 12 h and 24 h prediction horizons, respectively. So quantum computing also significantly reduced the grid stress during the peak time. Such optimization could not be achieved by commonly used traditional optimization methods. Therefore, for the complex day ahead time-of-use demand response scenarios, only quantum computing could achieve real-time MPC to minimize the electricity usage of the RTU and grid stress.

5. Discussion and future works

In this study, we used quantum computing to solve the optimization of energy-efficient model predictive control of RTU in the office building. We reformulated the optimization to the QUBO for the D-Wave quantum computer, which was the only commercial quantum computer available now. Currently, the architectures of quantum computing were still in the early stage of development that had limitations in the ease of computation, performance, and even algorithm. Only limited number of qubits and their coupling in the QPU could be used for direct embedding in D-Wave Advantage system. Large-scale problems still needed to be decomposed into many sub-problems to be solved. This required the assistance of traditional optimization algorithms; thus the computing time would increase. Some factors such as error correction, decoherence qubits, and limited quantum control lead to obstacles of accuracy of quantum computing and quantum computer. To improve the precision of optimization, increasing annealing time and spin reversal transform were feasible ways, but they would also lead to more computing time. What is more, quantum computing required reformulation of the original problem into a specific format, thus not all the optimization problems could be solved. If the objective function or constraint in the optimization problem is not a polynomial, but a fraction, radical expression, or contain special functions (e.g. exp, log, sin), then it cannot be reformulated into the form of Hamiltonian in Eq (1). Thus this optimization cannot be solved by a quantum computer easily. This is the current limitation of using a quantum computer to solve optimization. As long as the final objective function is polynomial, even for non-linear problems, quantum computers can solve it. We need further studies to take advantage of quantum computing for more complex problems. From an optimization perspective, annealing-based quantum computers were closer to discrete optimization problems than gate-model quantum computers [99]. This was because annealing was specifically built for optimization, whereas gate quantum computers followed general computing methods. Quantum computers for commonly used computing were still developing in the early stage. Finally, there was a huge cost for hardware and maintenance of the quantum computer. The energy required to run quantum computing may be higher than the optimized energy efficiency of the building HVAC system at this stage. Therefore, before quantum computing can become commonly practical, the issue of high cost must be addressed. In the future, it is anticipated that researchers can overcome the existing obstacles to make quantum computing play a greater role.

For the future work, there are few potential aspects: 1) optimize supply air temperature. Theoretically, it is possible to include supply air temperature as one of the continuous optimal variables, and additional energy savings will be expected. However, additional efforts on reformulation of the optimization equation are needed; 2) different polynomial formulations for the penalty function. Future work can also focus on various forms of penalty functions. Such variation will impact the optimization results. It will be interesting to compare and select the most suitable penalty function.

6. Conclusion

In this study, we proposed the methods based on quantum computing to solve the mixed-integer non-linear optimization of MPC for the building HVAC systems. This research led to the following conclusions:

1. The original MPC of RTU optimization as a non-linear problem with discrete variables could be formulated as the QUBO, so that quantum computers could solve it.
2. Using quantum computing, we could obtain the similar solution as using the traditional optimization methods with a short prediction horizon, and the control differences were less than 2 %. For a longer prediction horizon, the computing time of quantum computers for solving the optimization problem in this study was greatly reduced to less than 0.4 % of that by the traditional optimization methods. Only quantum computing could achieve real-time optimization and responding to the control signal within 15 min. The problem with more discrete optimized variables could take the advantage of quantum computing.
3. MPC optimized by the traditional optimization method and quantum computing could save the cooling load by 43.5 % and 42.9 % compared with on–off control, respectively.
4. Day-ahead real-time MPC by quantum computing could reschedule the electricity usage of the RTU to off-peak hours by 80 % and reduce the electricity bill by 21 %. Therefore, quantum computing had the potential to solve large-scale non-linear optimization problems for building energy systems.

CRediT authorship contribution statement

Zhipeng Deng: Conceptualization, Investigation, Resources, Methodology, Software, Validation, Visualization, Writing – original draft. **Xuezheng Wang:** Methodology. **Bing Dong:** Project administration, Supervision, Conceptualization, Funding acquisition, Investigation, Resources, Software.

Declaration of Competing Interest

The authors declare that they have no known competing financial interests or personal relationships that could have appeared to influence the work reported in this paper.

Data availability

Data will be made available on request.

Acknowledgment

This study was supported by the Collaboration for Unprecedented Success and Excellence (CUSE) Grant at Syracuse University under II-

3267-2022 and by the U.S. National Science Foundation under Award No. 1949372.

Appendix

Table A1
The values of the parameters of the RC model.

Parameter	Value
R_1	0.2
R_2	0.2
R_{win}	0.003
C_z	2.62e8
C_w	1.38e8

References

[1] Aoun C. The smart city cornerstone: Urban efficiency. Schneider Electric White Paper 2013;1:1–13.
[2] Hoornweg D, Sugar L, Trejos Gómez CL. Cities and greenhouse gas emissions: moving forward. Environ Urban 2011;23(1):207–27.
[3] U.S. EIA (Energy Information Administration). (2022). Total Energy Monthly Data. https://www.eia.gov/totalenergy/data/monthly/pdf/mer.pdf.
[4] U.S. EIA (Energy Information Administration) (2021), ANNUAL ENERGY OUTLOOK 2021 . https://www.eia.gov/pressroom/presentations/AEO2021_Release_Presentation.pdf.
[5] Rajith A, Soki S, Hiroshi M. Real-time optimized HVAC control system on top of an IoT framework. In: 2018 Third international conference on fog and mobile edge computing (FMEC). IEEE; 2018. p. 181–6.
[6] Georgiou GS, Christodoulides P, Kalogirou SA. Real-time energy convex optimization, via electrical storage, in buildings–A review. Renew Energy 2019;139:1355–65.
[7] Bazmi AA, Zahedi G. Sustainable energy systems: Role of optimization modeling techniques in power generation and supply—A review. Renew Sustain Energy Rev 2011;15(8):3480–500.
[8] O'Neill Z, Li Y, Williams K. HVAC control loop performance assessment: A critical review (1587-RP). Science and Technology for the Built Environment 2016;23(4):619–36.
[9] Hazyuk I, Ghiaus C, Penhouet D. Optimal temperature control of intermittently heated buildings using Model Predictive Control: Part I - Building modeling. Build Environ 2012;51:379–87.
[10] Camacho EF, Alba BC. Model Predictive Control (Advanced Textbooks in Control and Signal Processing). 2nd ed. Springer; 2004.
[11] Yao Y, Shekhar DK. State of the art review on model predictive control (MPC) in Heating Ventilation and Air-conditioning (HVAC) field. Build Environ 2021;200:107952.
[12] Dong B, Lam KP. A real-time model predictive control for building heating and cooling systems based on the occupancy behavior pattern detection and local weather forecasting. In: Building Simulation. Berlin Heidelberg: Springer; 2014. p. 89–106.
[13] Risbeck MJ, Maravelias CT, Rawlings JB. Real-time mixed-integer optimization for improved economic performance in HVAC systems. In: Computer Aided Chemical Engineering, Vol. 44. Elsevier; 2018. p. 33–42.
[14] Ghahramani A, Karvigh SA, Becerik-Gerber B. HVAC system energy optimization using an adaptive hybrid metaheuristic. Energ Buildings 2017;152:149–61.
[15] Mirakhorli A, Dong B. Occupancy behavior based model predictive control for building indoor climate—A critical review. Energ Buildings 2016;129:499–513.
[16] Goyal S, Barooah P, Middelkoop T. Experimental study of occupancy-based control of HVAC zones. Appl Energy 2015;140:75–84.
[17] Huang Y, Wang Y, Liu N. A two-stage energy management for heat-electricity integrated energy system considering dynamic pricing of Stackelberg game and operation strategy optimization. Energy 2022;244:122576.
[18] Li W, Wang S, Koo C. A real-time optimal control strategy for multi-zone VAV air-conditioning systems adopting a multi-agent based distributed optimization method. Appl Energy 2021;287:116605.
[19] Cabrera JA, Mintz Y, Pedrasa JR, Aswani A. Designing Real-Time Prices to Reduce Load Variability with HVAC. In: In 2018 Annual American Control Conference (ACC). IEEE; 2018. p. 6170–5.
[20] Risbeck MJ, Maravelias CT, Rawlings JB, Turney RD. Mixed-integer optimization methods for online scheduling in large-scale HVAC systems. Optim Lett 2020;14(4):889–924.
[21] Shaikh PH, Nor NBM, Nallagownden P, Elamvazuthi I, Ibrahim T. A review on optimized control systems for building energy and comfort management of smart sustainable buildings. Renew Sustain Energy Rev 2014;34:409–29.
[22] Schirrer A, Brandstetter M, Leobner I, Hauer S, Kozek M. Nonlinear model predictive control for a heating and cooling system of a low-energy office building. Energ Buildings 2016;125:86–98.
[23] Joe J, Karava P. A model predictive control strategy to optimize the performance of radiant floor heating and cooling systems in office buildings. Appl Energy 2019;245:65–77.
[24] Asad HS, Yuen RKK, Huang G. Multiplexed real-time optimization of HVAC systems with enhanced control stability. Appl Energy 2017;187:640–51.
[25] Ganesh HS, Fritz HE, Edgar TF, Novoselac A, Baldea M. A model-based dynamic optimization strategy for control of indoor air pollutants. Energ Buildings 2019;195:168–79.
[26] Hilliard T, Swan L, Qin Z. Experimental implementation of whole building MPC with zone based thermal comfort adjustments. Build Environ 2017;125:326–38.
[27] Brooks J, Kumar S, Goyal S, Subramany R, Barooah P. Energy-efficient control of under-actuated HVAC zones in commercial buildings. Energ Buildings 2015;93:160–8.
[28] Li L, Cao X, Wang P. Optimal coordination strategy for multiple distributed energy systems considering supply, demand, and price uncertainties. Energy 2021;227:120460.
[29] Bengea SC, Kelman AD, Borrelli F, Taylor R, Narayanan S. Implementation of model predictive control for an HVAC system in a mid-size commercial building. HVAC&R Research 2014;20(1):121–35.
[30] Serale G, Fiorentini M, Capozzoli A, Bernardini D, Bemporad A. Model predictive control (MPC) for enhancing building and HVAC system energy efficiency: Problem formulation, applications and opportunities. Energies 2018;11(3):631.
[31] Kim D, Braun JE. Model predictive control for supervising multiple rooftop unit economizers to fully leverage free cooling energy resource. Appl Energy 2020;275:115324.
[32] Liu S, Zhou C, Guo H, Shi Q, Song TE, Schomer I, et al. Operational optimization of a building-level integrated energy system considering additional potential benefits of energy storage. Protection and Control of Modern Power Systems 2021;6(1):1–10.
[33] Zhang X, Shi W, Li X, Yan B, Malkawi A, Li N. Decentralized temperature control via HVAC systems in energy efficient buildings: An approximate solution procedure. In: 2016 IEEE Global Conference on Signal and Information Processing (GlobalSIP). IEEE; 2016. p. 936–40.
[34] Su B, Wang S. An agent-based distributed real-time optimal control strategy for building HVAC systems for applications in the context of future IoT-based smart sensor networks. Appl Energy 2020;274:115322.
[35] Nizami MSH, Hossain MJ, Amin BR, Fernandez E. A residential energy management system with bi-level optimization-based bidding strategy for day-ahead bi-directional electricity trading. Appl Energy 2020;261:114322.
[36] Risbeck MJ, Maravelias CT, Rawlings JB, Turney RD. A mixed-integer linear programming model for real-time cost optimization of building heating, ventilation, and air conditioning equipment. Energ Buildings 2017;142:220–35.
[37] Cigler J, Prívara S, Váňa Z, Žáčeková E, Ferkl L. Optimization of predicted mean vote index within model predictive control framework: Computationally tractable solution. Energ Buildings 2012;52:39–49.
[38] Drgoňa J, Picard D, Helsen L. Cloud-based implementation of white-box model predictive control for a GEOTABS office building: A field test demonstration. J Process Control 2020;88:63–77.
[39] Koziel, S., & Yang, X. S. (Eds.). (2011). Computational optimization, methods and algorithms (Vol. 356). Springer.
[40] Aswani, A., Master, N., Taneja, J., Culler, D., & Tomlin, C. (2011). Reducing transient and steady state electricity consumption in HVAC using learning-based model-predictive control. Proceedings of the IEEE, 100(1), 240-253.
[41] Biegler LT, Grossmann IE. Retrospective on optimization. Comput Chem Eng 2004;28(8):1169–92.
[42] Finck C, Li R, Zeiler W. Economic model predictive control for demand flexibility of a residential building. Energy 2019;176:365–79.
[43] Yang S, Wan MP, Chen W, Ng BF, Dubey S. Model predictive control with adaptive machine-learning-based model for building energy efficiency and comfort optimization. Appl Energy 2020;271:115147.
[44] Kirkpatrick S, Gelatt Jr CD, Vecchi MP. Optimization by simulated annealing science 1983;220(4598):671–80.
[45] Afroz Z, Shafiullah GM, Urmee T, Shoeb MA, Higgins G. Predictive modelling and optimization of HVAC systems using neural network and particle swarm optimization algorithm. Build Environ 2022;209:108681.
[46] Kusiak A, Xu G, Tang F. Optimization of an HVAC system with a strength multi-objective particle-swarm algorithm. Energy 2011;36(10):5935–43.
[47] Reeves CR. Genetic algorithms. In: Handbook of metaheuristics. Boston, MA: Springer; 2010. p. 109–39.
[48] Ramos Ruiz G, Lucas Segarra E, Fernández Bandera C. Model predictive control optimization via genetic algorithm using a detailed building energy model. Energies 2018;12(1):34.
[49] Seong NC, Kim JH, Choi W. Optimal control strategy for variable air volume air-conditioning systems using genetic algorithms. Sustainability 2019;11(18):5122.
[50] Eshraghi A, Salehi G, Heibati S, Lari K. An enhanced operation model for energy storage system of a typical combined cool, heat and power based on demand response program: The application of mixed integer linear programming. Build Serv Eng Res Technol 2019;40(1):47–74.
[51] Lu L, Cai W, Chai YS, Xie L. Global optimization for overall HVAC systems—Part I problem formulation and analysis. Energ Conver Manage 2005;46(7–8):999–1014.
[52] Wu Y, Maravelias CT, Wenzel MJ, ElBsat MN, Turney RT. Predictive maintenance scheduling optimization of building heating, ventilation, and air conditioning systems. Energ Buildings 2021;231:110487.
[53] Rawlings JB, Patel NR, Risbeck MJ, Maravelias CT, Wenzel MJ, Turney RD. Economic MPC and real-time decision making with application to large-scale HVAC energy systems. Comput Chem Eng 2018;114:89–98.

[54] Banos R, Manzano-Agugliaro F, Montoya FG, Gil C, Alcayde A, Gómez J. Optimization methods applied to renewable and sustainable energy: A review. Renew Sustain Energy Rev 2011;15(4):1753–66.
[55] Bhandari B, Lee KT, Lee GY, Cho YM, Ahn SH. Optimization of hybrid renewable energy power systems: A review. International journal of precision engineering and manufacturing-green technology 2015;2(1):99–112.
[56] Barber KA, Krarti M. A review of optimization based tools for design and control of building energy systems. Renew Sustain Energy Rev 2022;160:112359.
[57] Kirchmair G, Vlastakis B, Leghtas Z, Nigg SE, Paik H, Ginossar E, et al. Observation of quantum state collapse and revival due to the single-photon Kerr effect. Nature 2013;495(7440):205–9.
[58] Montanaro A. Quantum algorithms: an overview. npj Quantum. Information 2016;2(1):1–8.
[59] Gill SS, Kumar A, Singh H, Singh M, Kaur K, Usman M, et al. Quantum computing: A taxonomy, systematic review and future directions. Software: Practice and Experience 2022;52(1):66–114.
[60] Shor PW. Algorithms for quantum computation: discrete logarithms and factoring. In: Proceedings 35th annual symposium on foundations of computer science. IEEE; 1994. p. 124–34.
[61] Grover, L. K. (1996, July). A fast quantum mechanical algorithm for database search. In Proceedings of the twenty-eighth annual ACM symposium on Theory of computing (pp. 212-219).
[62] Harrow AW, Hassidim A, Lloyd S. Quantum algorithm for linear systems of equations. Phys Rev Lett 2009;103(15):150502.
[63] Wiebe N, Braun D, Lloyd S. Quantum algorithm for data fitting. Phys Rev Lett 2012;109(5):050505.
[64] Kerenidis I, Landman J, Luongo A, Prakash A. q-means: A quantum algorithm for unsupervised machine learning. Adv Neural Inf Proces Syst 2019;32.
[65] Srivastava S, Sundararaghavan V. Box algorithm for the solution of differential equations on a quantum annealer. Phys Rev A 2019;99(5):052355.
[66] Boixo S, Albash T, Spedalieri FM, Chancellor N, Lidar DA. Experimental signature of programmable quantum annealing. Nat Commun 2013;4(1):1–8.
[67] Lucas A. Ising formulations of many NP problems. Front Phys 2014;5.
[68] Santoro GE, Tosatti E. Optimization using quantum mechanics: quantum annealing through adiabatic evolution. J Phys A Math Gen 2006;39(36):R393.
[69] Dorigo M, Birattari M, Stutzle T. Ant colony optimization. IEEE Comput Intell Mag 2006;1(4):28–39.
[70] Kadowaki T, Nishimori H. Quantum annealing in the transverse Ising model. Phys Rev E 1998;58(5):5355.
[71] Mukherjee S, Chakrabarti BK. Multivariable optimization: Quantum annealing and computation. The European Physical Journal Special Topics 2015;224(1):17–24.
[72] Ajagekar A, You F. Quantum computing for energy systems optimization: Challenges and opportunities. Energy 2019;179:76–89.
[73] Ajagekar A, You F. Quantum computing assisted deep learning for fault detection and diagnosis in industrial process systems. Comput Chem Eng 2020;143:107119.
[74] Ding Y, Chen X, Lamata L, Solano E, Sanz M. Implementation of a hybrid classical-quantum annealing algorithm for logistic network design. SN Computer Science 2021;2(2):1–9.
[75] Castillo J, Pena-Brage F. Optimization of a refinery scheduling process with column generation and a quantum annealer. Optim Eng 2021:1–18.
[76] Silva, F. F., Carvalho, P., Ferreira, L. A., & Omar, Y. (2021). A QUBO Formulation for Minimum Loss Spanning Tree Reconfiguration Problems in Electric Power Networks. arXiv preprint arXiv:2109.09659.
[77] Bhatia M, Sood SK. Quantum computing-inspired network optimization for IoT applications. IEEE Internet Things J 2020;7(6):5590–8.
[78] Speziali S, Bianchi F, Marini A, Menculini L, Proietti M, Termite LF, et al. Solving Sensor Placement Problems In Real Water Distribution Networks Using Adiabatic Quantum Computation. In: In 2021 IEEE International Conference on Quantum Computing and Engineering (QCE). IEEE; 2021. p. 463–4.
[79] Ajagekar A, Humble T, You F. Quantum computing based hybrid solution strategies for large-scale discrete-continuous optimization problems. Comput Chem Eng 2020;132:106630.
[80] Crawford, D., Levit, A., Ghadermarzy, N., Oberoi, J. S., & Ronagh, P. (2016). Reinforcement learning using quantum Boltzmann machines. arXiv preprint arXiv:1612.05695.
[81] Adachi, S. H., & Henderson, M. P. (2015). Application of quantum annealing to training of deep neural networks. arXiv preprint arXiv:1510.06356.
[82] Drgoňa J, Arroyo J, Figueroa IC, Blum D, Arendt K, Kim D, et al. All you need to know about model predictive control for buildings. Annu Rev Control 2020;50:190–232.
[83] Ishikawa H. Transformation of general binary MRF minimization to the first-order case. IEEE Trans Pattern Anal Mach Intell 2010;33(6):1234–49.
[84] Boros E, Hammer PL. Pseudo-boolean optimization Discrete applied mathematics 2002;123(1–3):155–225.
[85] WeatherMaster Single Packaged Rooftop, (2022). https://www.shareddocs.com/hvac/docs/1005/Public/0B/48_50GC-4-6-02PD.pdf.
[86] ASHRAE, (2013). Standard, 62.1. Ventilation for Acceptable Indoor Air Quality.
[87] Zhang X, Pipattanasomporn M, Rahman S. A self-learning algorithm for coordinated control of rooftop units in small-and medium-sized commercial buildings. Appl Energy 2017;205:1034–49.
[88] Fontenot H, Ayyagari KS, Dong B, Gatsis N, Taha A. Buildings-to-distribution-network integration for coordinated voltage regulation and building energy management via distributed resource flexibility. Sustain Cities Soc 2021;69:102832.
[89] Newman HM. Bacnet: the global standard for building automation and control networks. Momentum Press; 2013.
[90] D-Wave, (2022a). https://docs.dwavesys.com/docs/latest/handbook_reformulating.html.
[91] Humble TS, McCaskey AJ, Bennink RS, Billings JJ, D'Azevedo, E. F., Sullivan, B. D., & Seddiqi, H.. An integrated programming and development environment for adiabatic quantum optimization. Comput Sci Discov 2014;7(1):015006.
[92] D-Wave, (2022b). https://www.dwavesys.com/solutions-and-products/systems/.
[93] D-Wave, (2022c). https://docs.dwavesys.com/docs/latest/leap.html.
[94] ASHRAE, (2018). Guideline 36, High-Performance Sequences of Operation for HVAC Systems.
[95] Memon RA, Chirarattananon S, Vangtook P. Thermal comfort assessment and application of radiant cooling: a case study. Build Environ 2008;43(7):1185–96.
[96] Broadbent A, Kashefi E. Parallelizing quantum circuits Theoretical computer science 2009;410(26):2489–510.
[97] Kitaev, A., & Watrous, J. (2000, May). Parallelization, amplification, and exponential time simulation of quantum interactive proof systems. In Proceedings of the thirty-second annual ACM symposium on Theory of computing (pp. 608-617).
[98] PGE (2022). https://www.pge.com/tariffs/electric.shtml.
[99] Zahedinejad, E., & Zaribafiyan, A. (2017). Combinatorial optimization on gate model quantum computers: A survey. arXiv preprint arXiv:1708.05294.